



Outdoor Scene Synthesis in the Infrared Range for Remote Sensing Applications

Thierry Poglio, Eric Savaria, Lucien Wald

► To cite this version:

Thierry Poglio, Eric Savaria, Lucien Wald. Outdoor Scene Synthesis in the Infrared Range for Remote Sensing Applications. CISST'02: International Conference on Imaging Science, Systems, and Technology, Jun 2002, Las Vegas, Nevada, United States. pp.CD. hal-00395026

HAL Id: hal-00395026

<https://hal.science/hal-00395026>

Submitted on 14 Jun 2009

HAL is a multi-disciplinary open access archive for the deposit and dissemination of scientific research documents, whether they are published or not. The documents may come from teaching and research institutions in France or abroad, or from public or private research centers.

L'archive ouverte pluridisciplinaire **HAL**, est destinée au dépôt et à la diffusion de documents scientifiques de niveau recherche, publiés ou non, émanant des établissements d'enseignement et de recherche français ou étrangers, des laboratoires publics ou privés.

Outdoor Scene Synthesis in the Infrared Range for Remote Sensing Applications

Thierry Poglio

Ecole des Mines de Paris,
Groupe T&M,
Sophia Antipolis, 06904,
FRANCE

Eric Savaria

Alcatel Space Industries,
“ System Architecture Division”,
Cannes-la-Bocca, 06156,
France

Lucien Wald

Ecole des Mines de Paris,
Groupe T&M,
Sophia Antipolis, 06904,
FRANCE

Abstract—*This paper deals with a method of representation of landscape for the simulation of the behavior of an outdoor scene in the thermal infrared range, from 3 to 14 μm . The scene and objects are modeled in 3-D at very high spatial resolution of half a meter or so. The mesh is adapted to reproduce all the physical phenomena and their variations, according to their relative importance. The classical facet is no longer appropriate. A new quantity is introduced: the element. The element is defined as a part of an object. It is homogeneous with respect to material constitution and energy flux balance at a given instant. The mesh representing the scene is made of the union of the elements for the period of simulation of the temperature. All computations of fluxes and temperature are made on this mesh. Sufficient accuracy can be achieved by considering the most important physical phenomena to generate the elements. Shadow effect is the most important one. Influences of other phenomena are modeled by the mean of texture synthesis. In this paper, the method to define and generate elements is exposed, and an example is given, showing the efficiency of such a method to predict surface temperature, and afterward the irradiance of the scene.*

Keywords—*Image synthesis, thermal infrared, 3-D, outdoor scene, very high spatial resolution.*

1. Introduction

There is a strong rising interest in the simulation of the behavior of an outdoor scene in 3-D, in the thermal infrared range, from 3 to 14 μm . Various fields, coming under remote sensing applications, like meteorology, farming, or military information are concerned. Yet, such simulations of scenes with a sub-metric spatial

resolution are not available. Existing simulators that have been the object of publications are dedicated to specific applications, like the simulation of the thermal behavior of vehicles by Johnson [11], or the study of canopies by Guillevic [8] for instance. Jaloustre-Audouin [9] and [10] have developed a simulator of any type of landscape, working with a 2-D modeling of the scene. Those simulators cannot be used nor extended because of their very construction.

Changing meteorological conditions, different places, different landscapes, different times and different spectral bands should be simulated. A landscape synthesis method was selected in order to meet better these requirements. In the visible range, the objects are illuminated by sources. Radiosity methods, e.g. by Foley [5] or Watt [20], or hierarchical radiosity by Cohen [3] or Hanrahan [6] can be used to solve such problems in complex environments. In the infrared range, each entity reflects and emits fluxes. Reflection process occurs in a similar way than in the visible range. Emission occurs as a function of the surface temperature. This temperature depends on meteorological and geographical conditions and on material properties. The solar forcing leads to an increase in temperature, while heat transfer due to strong cold wind decreases the temperature. Materials exhibit different thermal conductivity and emissivity that impact on the radiative budget. Due to conduction process, temperature at a given instant depends on the in-depth temperature at the previous moments. The temperature of an entity is also a function of the temperature of the surrounding because of the

radiative, conductive and convective processes. Accordingly, the computation of the temperature of an entity requests the computation of the temperature of all the entities of the scene at the simulation time and the previous instants. Thus, an iterative method is used to compute all temperatures.

2. Specificity of the infrared range

2.1 The radiance balance equation

In the general case, the energy equilibrium for a set of radiating objects is expressed, independently on the wavelength, by the following equation [see Equation (1)]:

$$L(x, \theta_v, \varphi_v) = L_e(x, \theta_v, \varphi_v) + \int_{\Omega} f_r(x, \theta, \varphi, \theta_v, \varphi_v) L_i(x, \theta, \varphi) \cos \theta d\omega \quad (1)$$

Notations and definitions used here are those given by Sillion and Puech [18]. Additional information on transfer in global illumination can be found in Arvo [1].

- 1) $L(x, \theta_v, \varphi_v)$, $L_e(x, \theta_v, \varphi_v)$ and $L_i(x, \theta_v, \varphi_v)$ are respectively the radiance (in $\text{W.m}^{-2}.\text{sr}^{-1}$) leaving point x in the viewing direction (θ_v, φ_v) , the emitted radiance by point x in the same direction, and the incident radiance impinging the point x from direction (θ, φ) .
- 2) $f_r(x, \theta, \varphi, \theta_v, \varphi_v)$ is the Bidirectional Reflectance Distribution Function (*BDRF*). It describes the reflective properties of point x and is defined by Nicodemus [13].
- 3) Ω is the set of directions (θ, φ) in the hemisphere covering the surface at point x .

To simulate images in narrow or large spectral bands, spectral quantities have to be taken into account; it concerns both emitted and incident radiance, the *BDRF*, and the spectral response g of the instrument. Considering landscapes, objects can be considered as lambertian reflectors and emitters. Buildings made of metal or window glasses for instance only weakly meet this assumption. Assumption of the

isotropy of the directional parameters can be made. Using fluxes G , E , and B_j instead of radiance L , L_e and L_j , and expressing the environment of object i , the previous equation [see Equation (1)] becomes [see Equation (2)]:

$$G_{i, \lambda_1, \lambda_2} = \int_{\lambda_1}^{\lambda_2} g(\lambda) E_i(\lambda) d\lambda + \sum_{j=1}^N F_{ij} \int_{\lambda_1}^{\lambda_2} g(\lambda) \rho_i(\lambda) B_j(\lambda) d\lambda \quad (2)$$

F_{ij} is the form-factor and represents the rate of energy exchange between object i and object j . It can be computed using *e.g.* Schröder [17] or estimated by Wallace [19]. Equation (2) is solved with an iterative method; emission and reflection are computed at order k and Equation (2) is solved in a given spectral range. The radiosity method leads to a complex system of equations: one system per spectral sample in a given spectral range. In the general case, this method cannot be applied easily. It is used better when Equation (2) is integrated from zero to infinity, to compute energy flux balance impinging objects.

2.2 The iterative process used for infrared image synthesis

The main difficulty relating to Equation (2) is to compute the E_i term, corresponding to the self-emission of the object. This term can be expressed as the product of the emissivity ε_s of the object by the blackbody function L^{bb} at the temperature T_s [see Equation (3)]:

$$E_i(\theta_v, \varphi_v, \lambda) = \pi \varepsilon_s(\theta_v, \varphi_v, \lambda) L^{bb}(T_s, \lambda) \quad (3)$$

The surface temperature of the object has to be known to make the simulation. This temperature is governed by the heat equation [see Equation (4)], that can be written under thermodynamical conditions usually encountered in landscapes (no internal source):

$$\frac{\partial T}{\partial t} = \kappa \Delta T \quad (4)$$

where κ is the thermal diffusivity, and Δ is the laplacian operator. This equation may be solved

using *e.g.* the finite difference method [2] or the method proposed by Deardorff [4]. Due to thermal inertia, the knowledge of this temperature at t requests the temperature at the previous moment ($t-dt$). The in-depth temperature of the object, and the energy flux balance at the surface of the object are the two necessary boundary conditions required to solve this second-order differential equation.

Given an initial state, an iterative process is harnessed to compute surface temperature at the instant of simulation. The interactions between physical parameters, and their variations in time are modeled. Methods exist, developed by Johnson [12] or Jaloustre-Audouin [9] to compute these interactions and their changes in time. Because it is iterative, and because of the complexity of models used for the energy flux balance determination, this process is by far the longest in computation time.

During this process, the energy flux balance is varying at the surface of an object; it is not constant across each facet and is not varying in time in the same way. Considering *e.g.* the shadow variations, a facet homogeneous at t with respect to flux balance will not necessary be homogeneous at $t+dt$. The smallest entities representing the scene may be considered, voxels for instance. With voxels, entity is either sunny or shadowed. Problems rise with respect to the number of voxels multiplied by the computation time used for energy flux balance and temperature determination for a voxel. On a similar way, geometrical facets are heterogeneous with respect to boundary conditions; if computed on facet, surface temperature would not be physically relevant.

Taking into account variations in time of all the interactions differentiates the image synthesis in the infrared range from that in the visible domain. The synthesis methods used for the simulation of landscapes in short wavelengths do not need to reproduce the recent past of the landscape as it is observed in real infrared images. In this case, the landscape representation is usually a set of objects; each object is described by a set a facets on which the calculus are performed. The classical radiosity method can be used in such a case. In the thermal infrared range, it cannot, except for considering the radiosity method for each voxel and each time-step. An entity permitting to compute both temperatures at each instant during the process and the radiance leaving the scene has to be used.

3. The element: a physically-based entity

The element is the entity that exhibits homogeneous properties with respect to geometrical considerations, material constitution, and the occurring physical phenomena at each instant. Moreover, to reduce as many as possible the number of elements, and afterward the computational time, an element is defined as the largest entity included in a facet.

The element [see Figure 1] is a part of an object; it is a 3-D entity. Its external surface is flat and oriented. The in-depth constitution of the element is made of one or several layers of primary materials; for instance, a wall can be made of two layers: construction concrete and insulation. The element is homogeneous for boundary conditions, both internal and external. Regarding internal boundary, internal temperature is the same on each point of the boundary (at each time-step). For external boundary, element is defined as being homogeneous with respect to energy flux balance at each instant during the simulation process. The mesh is made of the union of elements for the period of simulation of temperature. To better understand the element concept, one may consider a facet; this facet is partly shadowed at the instant t . These portions of the facet are a preliminary set of elements, which will be subsequently subdivided by taking into account other phenomena and other instants.

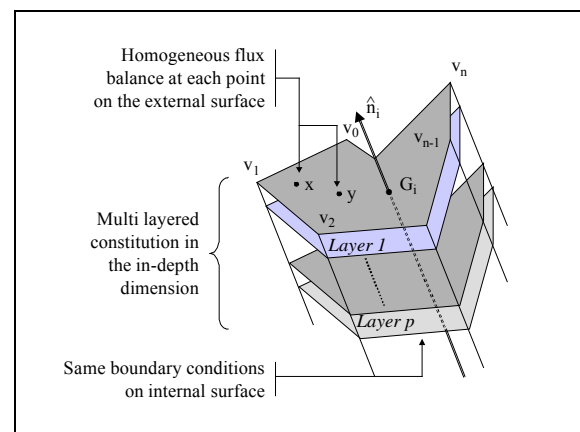


Figure 1—The multi-layered in-depth constitution of an element.

The landscape can be expressed in elements. Figure 2 shows the different steps used to construct the elements from the objects constituting the landscape. The simulator *OSIRIS* (Outdoor Scene InfraRed Image Simulator) [15] performs the element-based representation.

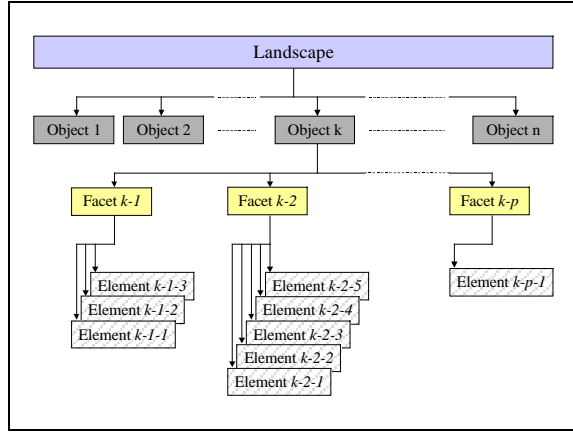


Figure 2—The landscape element representation.

4. The element generation

Sufficient accuracy can be achieved by considering the most important physical phenomena to generate the elements. Shadow effects are the most important ones [14]. In the present preliminary, influences of other phenomena are modeled by the means of texture synthesis.

4.1 The geometrical mesh generation

As a starting point, objects and facets representing the scene come from the concatenation of the geometrical and material

meshes. It gives rise to the initial mesh for discontinuity meshing approach [7]. For computation reasons, mesh is triangular. Identical areas with respect to boundary conditions split the scene in homogeneous areas. These areas, separated by boundaries, induce constraints on the initial mesh. A new mesh taking into account these constraints is achieved by the means of constrained triangulation. It is the geometrical support of the elements.

From the initial mesh, due to their orientation, shadowed facets at instant t are found. This subset of facets and the solar lighting direction define shadowed areas by projection on all other facets. Boundaries between shadowed and lit areas are constrained for the triangulation for the new mesh. Using Triangle software [16] a new mesh is obtained. Each entity of the mesh presents homogeneous properties with respect to sun illumination at instant t . This process is iterated [see Figure 3] to obtain the mesh for each instant during the simulation. The resulting mesh is the intersection of the meshes at each instant.

4.2 Managing the accuracy

The generation of such a mesh is based on physical considerations, which continuously change in time. There is no *a priori* limitation to the number of meshes. Nevertheless, a temporal time-step of 10 minutes had been chosen to compute temperature evolution when solving the heat equation [4]. Depending on the season, the geographical location of the scene, the height of the buildings and the moment in the day, shadow ground projections move slowly related to final pixel size.

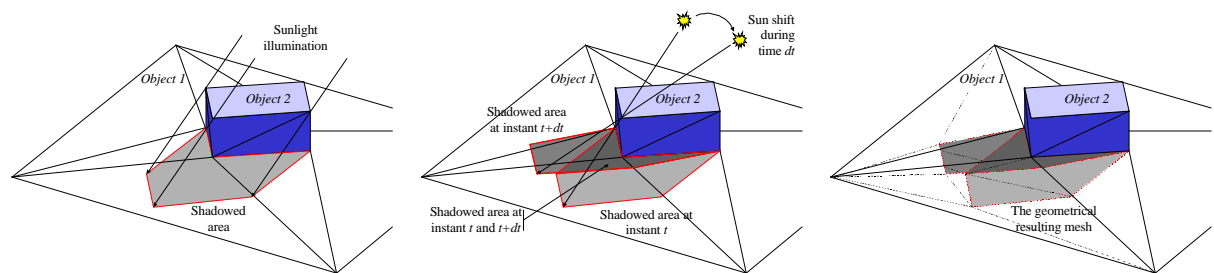


Figure 3—Illustration of the generation of the geometrical mesh.

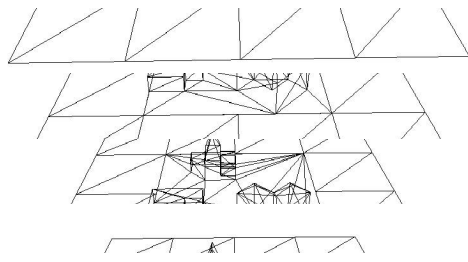


Figure 4-1–The 3-D model.

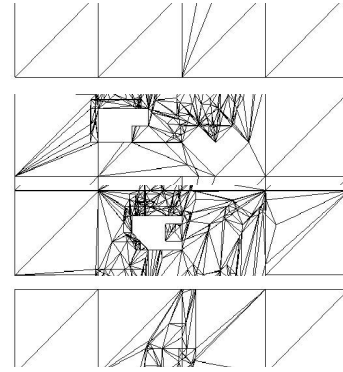


Figure 4-2–The element-based mesh.

Accordingly, the generation of shadow map is performed for each time-step when closing to the instant of simulation; the constraint is relaxed for the other instants. Similarly, considering spatial changes, relaxation criteria of the geometric accuracy can be applied on the constraints during the triangulation process in order to decrease the number of generated triangles. These criteria are related to the impact of the evolution of energy flux balance at the surface of the elements, and its impact on temperature change. Given an inaccuracy on boundary conditions, the farther away from the simulation time, the lower its impact. Several geometric criteria exist, which help to reduce the number of generated elements:

- 1) smallest triangles should not be considered. When the area of a triangle is smaller than a given area, and the longest edge of the triangle is shorter than a given length, this triangle is indivisible.
- 2) constraint points very close too each other are merged.
- 3) constraint points very close to vertex or edges are respectively confused with the vertex or their orthogonal projection on the edge.

Spatial and temporal relaxation criteria are put together. They are related to impacts of the temperature prediction due to variation of boundary conditions. The relaxation on both temporal and spatial criteria is performed till induced error is similar to that due to physical models. This permits to reduce the number of generated triangles, and afterward the computational time, while managing the accuracy of the temperature.

5. Results – OSIRIS simulations

To illustrate efficiency of the use of elements, an arbitrary 3-D scene was built, presenting buildings that project shadows. Discontinuity meshing are made to satisfy element definition criteria. For the sake of the simplicity, the example only shows the initial 3-D mesh [see Figure 4-1], and the ground mesh for four instants: 12, 14, 16 and 18 p.m. For visualization reason buildings are removed from Figure 4-2; only buildings overprints have been kept.

The simulation takes place in June, in Amiens in France (latitude: 49.54 N, longitude: 2.18 E). Houses are built with construction concrete, and an internal thermal insulation made of polystyrene. The central area is a car park made of asphalt, and the square enclosing this park is a bare soil. The three following images [see Figure 5-1, Figure 5-2 and Figure 5-3] are simulated at 6 p.m., after a sunny day, and after shadows swept out the entire scene. Images are viewed with a zenith angle of 20 °, and an azimuth angle of 60 ° East.

Figure 5-1 represents the surface temperature ranging from 14 °C in the shadow of the facade (black tones) to 33 °C for sunlit roof (white tones). Figure 5-2 and Figure 5-3 represent radiance respectively in band II and in band III. Reflection process dominates the signal in band II, whereas emission process dominates in band III. This explains that in band II contrasts are higher between shadowed and sunlit areas. In band II [see Figure 5-2], signal ranges approximately from 1.2 to 2.8 W.m².sr⁻¹. In band III [see Figure 5-3], signal ranges from 31.5 to 40.2 W.m².sr⁻¹.

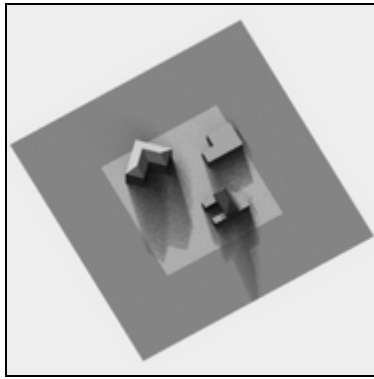


Figure 5-1—The surface temperature.

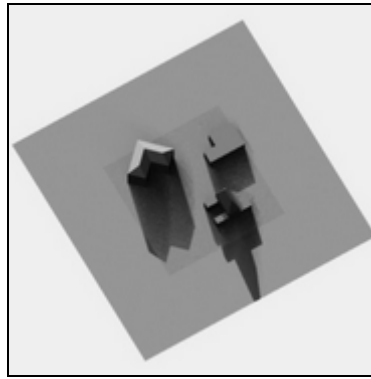


Figure 5-2—Radiance in band II (from 3 to 5 μm).

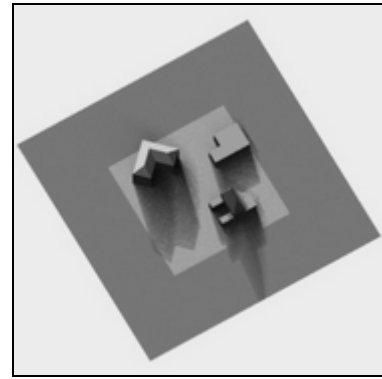


Figure 5-3—Radiance in band III (from 8 to 12 μm).

Thermal shadows at 6 p.m. are clearly visible, as well as temporal remanence of shadows. This is a typical effect of the infrared range. Simulations exhibit continuous variations of radiometry in the areas previously shaded. This is due to thermal inertia. It is emphasized on the bare soil, due to the high capacity of this material to store energy. The use of elements permits to well reproduce the temporal evolution of physical phenomena. This is necessary in this spectral range, where the scene keeps track of the recent past of boundary conditions. With the use of elements image is not photorealistic: textures have to be added. Texture expresses radiometric variations existing inside a given area supposed to be homogeneous. It can be synthesized considering the spatial variability of optical and thermal parameters of each material. For instance, this variability can be deduced from a visible image for optical parameters, and randomly chosen for thermal parameters, accordingly with real physical variations. Texture mapping comes under improvements before its integration in the *OSIRIS* simulator. Another possible improvement is an automatic search of spatial and temporal relaxation criteria. For the moment, the user has to give these criteria before performing the simulation.

6. Conclusion

In the thermal infrared range, radiance depends strongly on the surface temperature, itself also highly dependent on boundary conditions existing at the surface of the object. In this respect, the modeling of the landscape

should reproduce this carefully, in order to perform simulation with a maximum of physical realism. To achieve such a simulation, the elements were designed. They are homogeneous entities with respect to geometry, material and temporal evolution of physical phenomena. Physics can thus be taken into account accurately and the behavior of the landscape can be simulated precisely. Results presented here are the first obtained with the use of such a representation; they have to be assessed with help of real images related to the ground truth. These preliminary experiments have shown the relevance of such a methodology. Unavoidably, it requests considerable efforts in landscape modeling, software development and computational resources, compared to simulation in the visible range.

Acknowledgments

This research was performed under a grant of A.N.R.T., Ministry of Research in France. Thanks also go to J.R. Shewchuk for the use of the software Triangle, the 2-D quality mesh generator and Delaunay triangulator.

References

- [1] Arvo, J., "Transfer equation in global illumination." Global illumination, SIGGRAPH'93 Course Notes, no. 42, 1993.
- [2] Ciarlet, P.G., and Lions, J.L., *Handbook of Numerical Analysis*, Elsevier Science Publisher B.V., ISBN 0-444-70366-7, 1990.

- [3] Cohen, M., Grenberg, D.P., Immel, D.S., and Brook, P.J., "An efficient radiosity approach for realistic image synthesis," *IEEE Computer Graphics and Applications*, vol. 6, no. 3, pp 26-35, 1986.
- [4] Deardorff, J.W., "Efficient prediction of ground surface temperature and moisture with inclusion of a layer of vegetation," *Journal of Geophysical Research*, vol. 83, no. C4, pp 1889-1902, 1978.
- [5] Foley, J.D., van Dam, A., Feiner, S. K., and Hughes, J. F., *Computer Graphics, Principles and Practice. Second Edition in C*. Addison-Wesley Publishing Company, ISBN 0-201-84840-b, 1996.
- [6] Hanrahan, P., Salzman, D., and Aupperle, L., "A rapid hierarchical radiosity algorithm," *Computer Graphics, SIGGRAPH'91 Proceedings*, vol. 25, no. 4, pp 197-206, 1991.
- [7] Heckbert, P.S., "Discontinuity meshing for Radiosity," *Proceedings of the Third Eurographics Workshop on Rendering*, pp 203-216, 1992.
- [8] Guillevic, P., "Modélisation des bilans radiatif et énergétique des couverts végétaux." Thèse de Doctorat, Université P. Sabatier, Toulouse, France, 1999.
- [9] Jaloustre-Audouin, K., "SPIrou : Synthèse de Paysage en InfraRouge par modélisation physique des échanges à la surface." Thèse de Doctorat, Université de Nice-Sophia Antipolis, Nice, France, 1998.
- [10] Jaloustre-Audouin, K., Savaria, E., and Wald, L., "Simulated images of outdoor scenes in infrared spectral band." *AeroSense'97*, SPIE, Orlando, 1997.
- [11] Johnson, K., Curran, A., Less, D., Levanen, D., Marttila, E., Gonda, T., and Jones, J., "MuSES: A new heat and signature management design tool for virtual prototyping," *Proceedings of the 9th Annual Ground Target Modelling & Validation Conference*, Houghton, MI, 1998.
- [12] Johnson, K.R., Wood, S.B., Rynes, P.L., Yee, B.K., Burroughs, F.C., and Byrd, T., "A methodology for rapid calculation of computational thermal models," *SAE International Congress & Exposition, Underhood Thermal Management Session*, Detroit, Michigan, 1995.
- [13] Nicodemus, F.E., Richmond, J.C., and Hsia, J.J., *Geometrical considerations and nomenclature for reflectance*, NBS Monograph 160, U.S. National Bureau of Standards, Washington, D.C, 1977.
- [14] Poglio, T., Savaria, E., and Wald, L., "Influence of the three-dimensional effects on the simulation of landscapes in thermal infrared," *Proceedings of the 21st Symposium EARSel*, Marne-la-Vallée, France, pp 133-139, 2001.
- [15] Poglio, T., Savaria, E., and Wald, L., "Specifications and conceptual architecture of a thermal infrared simulator of landscapes," *Proceedings of the Sensors, Systems, and Next Generation Satellites VII, 8th International Symposium on Remote Sensing*, SPIE, Toulouse, France, vol. 4540, pp 488-497, 2001.
- [16] Shewchuk, J.R., "Triangle: Engineering a 2D Quality Mesh Generator and Delaunay Triangulator," *First whorshop on Applied Computational Geometry*, Philadelphia, ACM, pp 124-133, 1996.
- [17] Schröder, P., and Hanrahan, P., "On the form factor between two polygons," *Computer Graphics Proceedings, Annual Conference Series: SIGGRAPH'93* (Anaheim, CA), ACM SIGGRAPH, New York, pp 163-164, 1993.
- [18] Sillion, F.X., and Puech, C., *Radiosity & Global Illumination*. Morgan Kaufmann Publishers, Inc., ISBN 1-558-60277-1, San Francisco, CA, U.S.A., 1994.
- [19] Wallace, J.R., Elmquist, K.A., and Haines, E.A., "A ray tracing algorithm for progressive radiosity," *Computer Graphics*, vol. 23, no. 3, pp 315-324, 1989.
- [20] Watt, A., *3-D Computer Graphics*, Third Edition, Addison-Wesley Publishing Compagny Inc, ISBN 0-201-39855-9, 2000.